Leukemia (2007) 21, 2153–2163

www.nature.com/leu

ORIGINAL ARTICLE

Combined single nucleotide polymorphism-based genomic mapping and global gene expression profiling identifies novel chromosomal imbalances, mechanisms and candidate genes important in the pathogenesis of T-cell prolymphocytic leukemia with inv(14)(q11q32)

J Dürig[1], S Bug[2], L Klein-Hitpass[3], T Boes[4], T Jöns[5], JI Martin-Subero[2], L Harder[2], M Baudis[6], U Dührsen[1] and R Siebert[2]

[1]Department of Hematology, University Hospital, University of Duisburg-Essen, Essen, Germany; [2]Institute of Human Genetics, University Hospital Schleswig-Holstein, Campus Kiel, Kiel, Germany; [3]Institute of Cell Biology, University Hospital, University of Duisburg-Essen, Essen, Germany; [4]Institute for Medical Informatics, Biometry and Epidemiology, University Hospital, University of Duisburg-Essen, Essen, Germany; [5]Institute of Integrative Anatomy, Humboldt-University Berlin, Charité, Germany and [6]Institute of Human Genetics, Medical Faculty RWTH, University Hospital Aachen, Aachen, Germany

T-cell prolymphocytic leukemia (T-PLL) is a rare aggressive lymphoma derived from mature T cells, which is, in most cases, characterized by the presence of an inv(14)(q11q32)/t(14;14)(q11;q32) and a characteristic pattern of secondary chromosomal aberrations. DNA microarray technology was employed to compare the transcriptomes of eight immunomagnetically purified CD3+ normal donor-derived peripheral blood cell samples, with five highly purified inv(14)/t(14;14)-positive T-PLL blood samples. Between the two experimental groups, 734 genes were identified as differentially expressed, including functionally important genes involved in lymphomagenesis, cell cycle regulation, apoptosis and DNA repair. Notably, the differentially expressed genes were found to be significantly enriched in genomic regions affected by recurrent chromosomal imbalances. Upregulated genes clustered on chromosome arms 6p and 8q, and downregulated genes on 6q, 8p, 10p, 11q and 18p. High-resolution copy-number determination using single nucleotide polymorphism chip technology in 12 inv(14)/t(14;14)-positive T-PLL including those analyzed for gene expression, refined chromosomal breakpoints as well as regions of imbalances. In conclusion, combined transcriptional and molecular cytogenetic profiling identified novel specific chromosomal loci and genes that are likely to be involved in disease progression and suggests a gene dosage effect as a pathogenic mechanism in T-PLL.
Leukemia (2007) **21,** 2153–2163; doi:10.1038/sj.leu.2404877; published online 16 August 2007
Keywords: T-cell prolymphocytic leukemia (T-PLL); genomic aberrations; uniparental disomy; cDNA microarray analysis

Introduction

T-cell prolymphocytic leukemia (T-PLL) is a rare lymphoproliferative disease with distinctive clinical, morphologic, immunophenotypic and cytogenetic characteristics.[1–3] Most T-PLLs exhibit a mature post-thymic CD2+, CD3+, CD7+, CD4+, CD8− immunophenotypes, but CD4+, CD8+ and CD4−, CD8+ cases are also commonly seen.[1,2] The disease follows an aggressive clinical course in most patients with median survival times ranging from 7 to 30 months.[1,2] The leukemic cells are generally resistant to alkylating drugs, and the most promising treatment results are currently achieved using chemoimmunotherapy protocols combining the anti-CD52 monoclonal antibody alemtuzumab with fludarabine, anthracyclines and alkylating agents.[1,2,4,5]

The genetic hallmark of T-PLL is the inversion inv(14)(q11q32) or its variant, the translocation t(14;14)(q11;q32), which are present in up to 80% of the cases.[1,3,6] These rearrangements juxtapose enhancer elements of the TCRAD locus in 14q11 next to oncogenes located within the TCL1 locus in 14q32, whose expression is then deregulated.[7–9] Besides the inv(14), which is regarded as the primary oncogenic event in T-PLL,[7–10] the tumor cells usually harbor a high load of additional chromosomal aberrations.[3,6] These secondary chromosomal aberrations include overrepresentations of 8q and deletions of 8p, frequently due to formation of an isochromosome iso(8q),[3,6] as well as losses on chromosome 11,[11,12] and with lower frequency involving other chromosomal regions like 22q and 6q.[3] Although this pattern of secondary changes in inv(14)/t(14;14)-positive T-PLL is highly conserved and characteristic of T-PLL,[3] the target genes of the recurrent secondary aberrations in this disease are largely unknown, except ATM, which is supposed to be the tumor suppressor gene in the commonly deleted region in 11q22∼23.[11,12]

In various subtypes of leukemias and lymphomas, array-based transcriptional profiling recently identified characteristic gene expression signatures.[13–15] Moreover, comparative cytogenetic analyses showed these gene expression profiles to be closely related to the presence of recurrent chromosomal changes.[13–16] To investigate further the molecular pathogenesis of T-PLL, here we performed gene expression profiling (GEP) on purified CD3+ cells of five fluorescence *in situ* hybridization (FISH)-verified inv(14)t(14;14)-positive T-PLL diagnosed according to the World Health Organization (WHO) criteria[17] and eight age-matched healthy donors using the Affymetrix U133A microarray platform. To identify candidate genes with potential relevance to the disease process, GEP results were then correlated with genomic aberrations detected by FISH and high-density single nucleotide polymorphism (SNP)-based mapping.

Materials and methods

In silico *comparative analysis of chromosomal imbalances in T-PLL*

In silico comparative analysis of chromosomal imbalances in 67 cytogenetically characterized T-PLL with unequivocal descrip-

Correspondence: Dr J Dürig, Department of Hematology, University Hospital, Hufelandstr 55, 45122 Essen, Germany.
E-mail: jan.duerig@uk-essen.de
Received 15 January 2007; revised 18 June 2007; accepted 19 June 2007; published online 16 August 2007

tion of a t/inv(14;14)(q11;q32) obtained from the Mitelman Database of Chromosome Aberrations in Cancer (http://cgap.nci.nih.gov/Chromosomes/Mitelman) was performed using the Progenetix software as previously described (www.progenetix.net[18,19]).

Patients and sample preparation

The overall experimental strategy pursued in this study is shown in Supplementary Figure 1. A total of 13 samples were selected for this study, in which the diagnosis of T-PLL was established according to the WHO criteria.[17] Only T-PLLs were included, in which standard chromosome analysis on short-term cultures of the tumor cells using fluorescence R-banding revealed an aberrant karyotype including the typical inv(14)/t(14;14). Patient characteristics including full karyotypes are given in Supplementary Table 1. Fresh material for combined gene expression and genomic profiling was available from five patients with T-PLL (T-PLL1–T-PLL5, Supplementary Table 1). In seven patients (T-PLL6, T-PLL12) only material for genomic analyses was available. Peripheral blood cells from eight healthy donors served as controls. One T-PLL lacking inv(14)/t(14;14) (patient A, Supplementary Table 1) served as an additional (negative) control for comparative analysis of gene expression changes linked to inv(14)/t(14;14) and was also included in the flow cytometric analysis of CD35 expression (see below). All samples were obtained with informed consent from the files of the Department of Hematology, University Hospital Essen, and the Institute of Human Genetics, University Hospital Schleswig-Holstein, Campus Kiel. The study was approved by the ethics committee of the faculty of medicine at the University of Duisburg-Essen.

Mononuclear cells were isolated from fresh peripheral blood samples (Lymphoprep, Invitrogen, Karlsruhe, Germany). CD3+ T cells were enriched employing anti-CD3 magnetic microbeads (MidiMacs, Miltenyi Biotec, Bergisch Gladbach, Germany) resulting in a purity of CD3+ T cells of >90% by flow cytometry.

GEP and statistical analysis of gene expression data

GEP was performed on RNA from 1 to 2×10^8 CD3+ cells (RNeasy midi kit, Qiagen, Hilden, Germany) using the Affymetrix U133A microarray platform as recently described.[20] Differentially expressed genes (Supplementary Table 2) were identified using non-parametric Mann–Whitney U-test and the significance analysis of microarrays method[21] in a supervised approach as described in the legend of Supplementary Table 2. The panel of differentially expressed genes was further functionally analyzed for enrichment in the gene ontology (GO) categories 'biological process' and 'molecular function' employing the GO stat tool (Supplementary Table 3).[22] Furthermore, differentially expressed genes (Supplementary Table 2) were tested for nonrandom distribution to individual chromosome arms employing the hypergeometric distribution method[23] to identify candidate regions for genomic aberrations (Table 1). With this distribution, the probability of observing at least x probe sets, which represent genes located on one chromosome is given by

$$P(N,K,n,x) = 1 - \sum_{i=0}^{x-1} \frac{\binom{K}{i}\binom{N-K}{n-i}}{\binom{N}{n}}$$

where N is the number of probe sets with known chromosomal location (here 19416), n the number of differentially expressed probe sets with known chromosomal location (here 830) and K the number of probe sets, which represent genes located on the respective chromosome. To calculate the P-values, the statistical software SAS version 8.02 was used. Chromosomal locations of the respective genes were derived from the annotation table provided by Affymetrix at http://www.affymetrix.com. Gene expression changes were then correlated with chromosomal imbalances as detected by Affymetrix GeneChip 50 K SNP array and FISH analysis (see below). The raw experimental data can be accessed through http://www.ncbi.nlm.nih.gov/geo/.

Genome mapping using SNP arrays and FISH

Interphase FISH probes and results. Interphase FISH was performed on cell suspensions left from cytogenetic analysis. Probe selection, preparation, labeling and hybridization procedures followed recently described protocols.[24] Supplementary Table 4 summarizes the applied probes and results. For each hybridization, at least 100 cells were evaluated whenever possible. FISH results are presented in analogy to International System for Human Cytogenetic Nomenclature 1995.[25]

GeneChip analyses. GeneChip analyses were conducted as recently described.[26] Genomic DNA (extracted with QIAamp DNA Blood Midi Kit, Qiagen, Hilden, Germany) was subjected to Affymetrix GeneChip 50K SNP *Xba*I mapping array analyses following the standard protocol for Affymetrix GeneChip Mapping 100 K arrays (Affymetrix Inc., Santa Clara, CA, USA). Arrays were evaluated using the Affymetrix software tools

Table 1 Hypergeometric distribution analysis of T-PLL vs normal donor T-cell distinction genes for enrichment (clustering) on individual chromosome arms (see Materials and methods for statistical details)

Chromosome	*Number of upregulated probe sets*	*Number of downregulated probe sets*	*Number of probe sets present on chromosomal arm*	P-*value upregulated probe sets*	P-*value downregulated probe sets*
chr8q	40	1	402	0.00001	0.999402
chr6p	30	6	753	0.000316	0.99402
chr1p	32	21	1116	0.028121	0.46073
chr8p	9	12	308	0.169904	0.010818
chr10p	2	12	168	0.484262	0.00006
chr14q	12	20	696	0.746663	0.02927
chr11q	10	31	739	0.931152	0.00001
chr6q	5	21	429	0.970977	0.000247
chr18p	0	8	94	1	<0.001

Abbreviation: T-PLL, T-cell prolymphocytic leukemia.

(GDAS, v3.0; CNAT2.0) and according to the criteria we established based on FISH-validated copy-number aberrations (see legends to Supplementary Table 5 and Supplementary Figure 2 in Supplementary Materials).

Flow cytometric analysis of CR1/CD35

CR1/CD35 expression on the surface of T-PLL and normal donor (ND)-derived peripheral blood T cells was determined by two-color flow cytometry employing directly fluorochrome-labeled antibodies at pre-tested optimal concentrations. In brief, freshly thawed peripheral blood mononuclear cells (PBMNCs) from patients with T-PLL ($n=7$) and normal controls ($n=10$) were stained with anti-CD3-phycoerythrin (PE, Becton Dickinson, Heidelberg, Germany) and anti-CR1/CD35-fluorescein isothiocyanate (FITC; Immunotech, Marseille, France). Negative isotype-matched controls (Becton Dickinson) were used to define the threshold line separating surface marker positive and negative cells such that less than 1% of isotype-positive cells were present to the right of the line. The relative density of CR1/CD35 on lymphocyte-gated CD3 + T cells was quantified by determining the mean fluorescent intensity (MFI) for FITC and subtracting the corresponding MFI values of the control antibody. The CR1/CD35 expression levels of individual T-PLL patients and healthy controls (ND) are plotted as geometric means.

Immunoblot analysis of ankyrin-1

T-PLL cells, ND PBMNCs and Jurkat cells were homogenized in a hypotonic Tris/HCl buffer. The 1000 g supernatant was centrifuged for 20 min at 100 000 *g* and the resulting pellets were resuspended. After determination of the protein concentration, an equal amount, representing 25 μg per lane, was subjected to sodium dodecyl sulfate–polyacrylamide gel electrophoresis. Electrophoretically separated proteins were transferred to nitrocellulose membranes and incubated with phosphate-buffered saline (PBS) containing 10% milk powder to block unspecific protein-binding sites. Thereafter, stripes were incubated for 16 h at 4°C with an antiserum directed against human ankyrin in appropriate dilution in PBS/10% milk powder as previously described.[27] Washing steps were performed with PBS containing 0.05% Tween-20. The bound immunoglobulins were incubated with horse radish peroxidase (HRP)-labeled antiserum raised against rabbit immunoglobulin G and chemoluminescence was visualized using the enhanced chemiluminescence (ECL) detection system (Amersham Braunschweig, Germany). As a positive control, human erythroid membranes (human ghosts, HGs) were used.[27]

Results

In silico *comparative analysis of chromosomal imbalances T-PLL cases*

Figure 1a shows an *in silico* comparative analysis[18,19] of 67 cytogenetically characterized T-PLL cases with unequivocal description of a t/inv(14;14)(q11;q32) obtained from the Mitelman Database of Chromosome Aberrations in Cancer (http://cgap.nci.nih.gov/Chromosomes/Mitelman). Highly recurrent secondary changes as detected by standard metaphase cytogenetics include overrepresentations of 8q and deletions of 8p, frequently due to formation of an isochromosome iso(8q), as well as losses on chromosome 11 and with lower frequency involving other chromosomal regions like 22q and 6q. Figure 1b shows the profiles of 31 T-PLL cases analyzed by comparative genomic hybridization (CGH), derived from the Progenetix database (www.progenetix.net). In the cases analyzed by CGH (Figure 1b), additional genomic imbalances such as gains on 6p, 14qter and 22q, and more clearly delimited regional changes like a deletion hot spot in 11q22 ~q23 are apparent.

GEP

The transcriptomes of CD3-purified cells from the peripheral blood of five inv(14)-positive T-PLL cases were compared with those of eight ND-derived immunomagnetically purified peripheral blood T-cell samples using the Affymetrix U133A platform (Supplementary Figure 1).

Applying the filter and evaluation strategies outlined in Supplementary Figure 1 and in Materials and methods, supervised comparative analysis revealed that a total of 435 probe sets (392 genes) were significantly upregulated and 395 probe sets (342 genes) were significantly downregulated in the T-PLL samples (Supplementary Table 2) as compared to the normal controls.

Deregulation of genes directly linked to inv(14)/t(14;14). Among the genes significantly upregulated in the T-PLL samples was TCL1A located at the TCL1 locus in 14q32.1. In line with previous reports[8,9] and despite the FISH-proven presence of inv(14)/t(14;14) in all five T-PLL samples studied, no consistent upregulation of the genes TCL1B, TNG1 or TNG2 at the TCL1 locus was observed (Figure 2). However, in one-fifth of T-PLL samples, TNG1 was found to be unequivocally upregulated, whereas its expression was absent in all of the remaining T-PLL cases and the normal controls (Figure 2). Conversely, an inv(14)/t(14;14)-negative T-PLL sample (patient A, see Supplementary Table 1) lacked overexpression of TCL1A or any other gene at the TCL1 locus (Figure 2). Expression from the TCRAD locus in 14q11 was decreased in all T-PLL samples (Supplementary Table 2). Residual expression of TCRA detectable in all five T-PLL most likely originated from the TCRAD locus not involved in the inv(14)/t(14;14).[28,29]

Molecular pathway analysis of GEP data and identification of genes with potential importance for the pathogenesis of T-PLL. To elucidate further the biological processes and molecular pathways deregulated in T-PLL, the panel of differentially expressed genes (Supplementary Table 2) was functionally analyzed for enrichment in the GO categories 'biological process' and 'molecular function' employing the GO stat tool.[22] This analysis revealed significant enrichment of genes comprised in the 'cell surface receptor-linked signal transduction', 'defense response' and 'immune response' GO-biological process, and 'receptor activity' and 'transmembrane receptor activity' GO-molecular function categories (Supplementary Table 3), respectively. Several of the genes upregulated in T-PLL are involved in regulation of transcription, nucleosome assembly, translation and cell cycle control (for example, Nijmegen breakage syndrome 1 (NBS1), TCF7L, CCNB2, CCNB1, CCNG2, PFAS, PAICS, HIST1H2AE, HIST1H2B, HIST1H4G, ELF4EBP1, ELL3). In contrast, various pro-apoptotic genes like FAS, CASP1, CASP4, CASP8, STK17A and TRAIL were down-modulated (Supplementary Table 2). This expression pattern might provide the leukemic cells with an increased proliferative drive and reduced susceptibility to apoptotic cell death, thus explaining the aggressive clinical behavior of these cells *in vivo*. Similarly, deregulation of the insulin-like growth factor (IGF) system

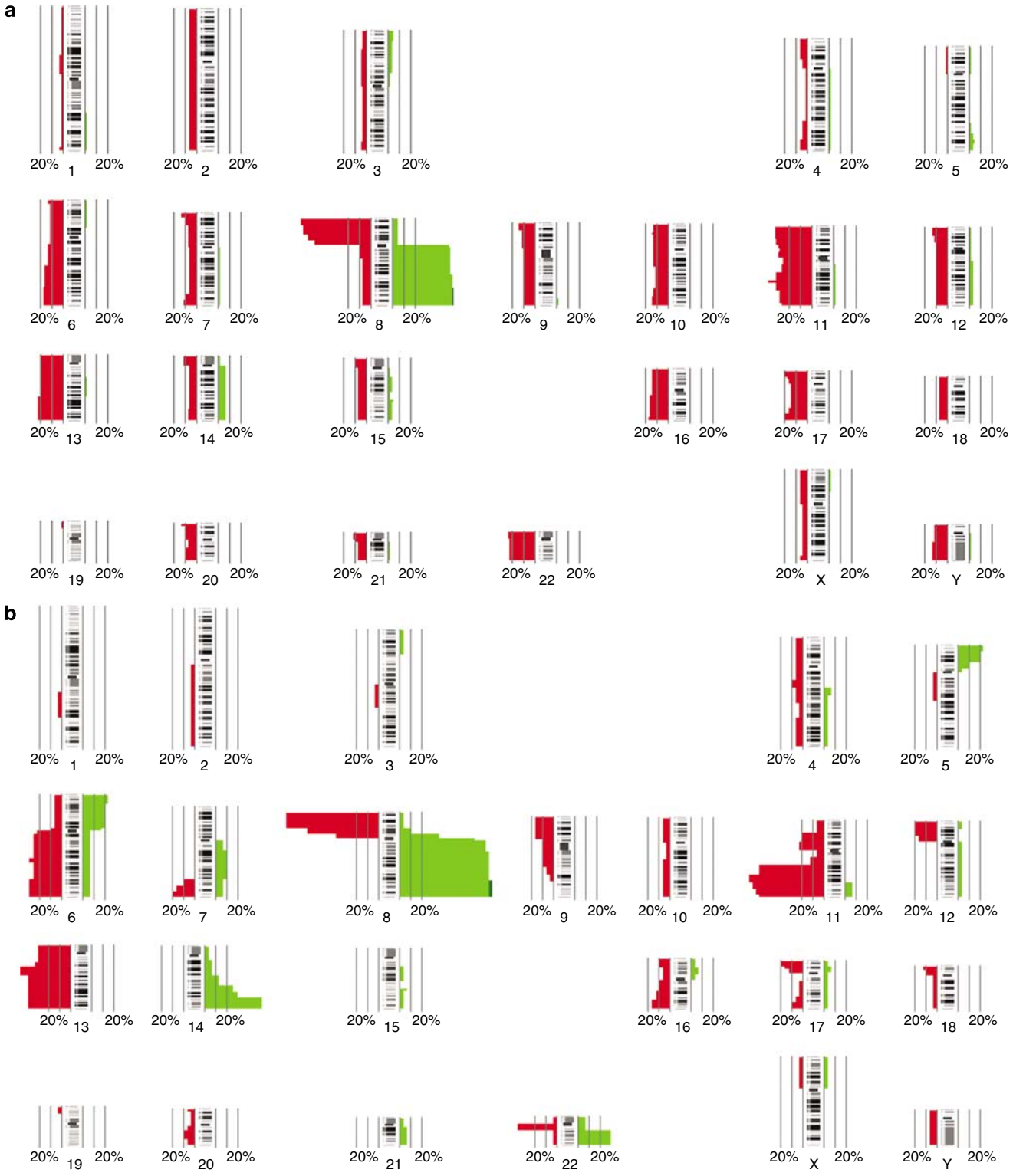

Figure 1 *In silico* comparative analysis of chromosomal imbalances in 67 cytogenetically characterized T-PLL cases (**a**) with unequivocal description of a t/inv(14;14)(q11;q32) obtained from the Mitelman Database of Chromosome Aberrations in Cancer (http://cgap.nci.nih.gov/Chromosomes/Mitelman).[19] (**b**) Profiles of 31 T-PLL cases analyzed by comparative genomic hybridization (CGH), derived from the Progenetix database (www.progenetix.net;[18,19]). For most of these cases, no information about structural chromosomal abnormalities was available. The output gives a summary of the imbalances determined by conventional cytogenetics (**a**) or CGH (**b**) as percentage of cases in the data set, showing the respective change on the corresponding band. A loss of genomic material is indicated by an amplitude to the left and colored in red, a gain of genomic material is marked by an amplitude to the right and green color. As per convention,[3] chromosomal regions that were involved in more than 20% of the cases analyzed were referred to as recurrent.

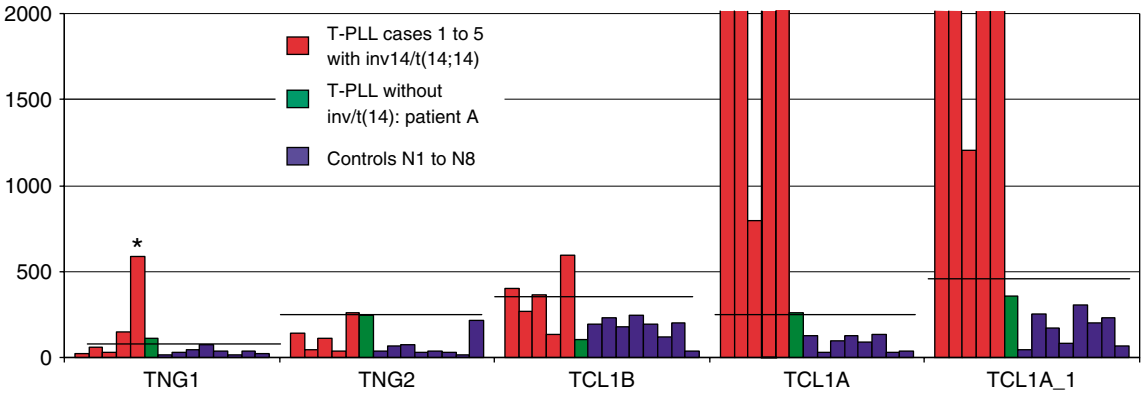

Figure 2 Microarray-based gene expression profiling (GEP) of genes residing at the TCL1 locus in 14q32. Expression levels of CD3-purified cells of five T-PLL cases are shown in red, the expression levels of a T-PLL sample without a inv(14)/t(14;14) (patient A, Supplementary Table 1) is shown in green and expression levels of CD3-purified cells of eight normal controls are shown in blue. Normalized expression units are plotted on the *y* axis. Significance of variation in expression is given by a threshold, which is defined as the mean value of expression in all controls plus three times the standard deviation of these values and is marked in the graph by horizontal lines. Note, none of the following genes, that is TNG1, TNG2, TCL1B was called present by the Affymetrix algorithm in any of the 13 samples analyzed except TNG1 in T-PLL 5, which is marked by an asterisk.

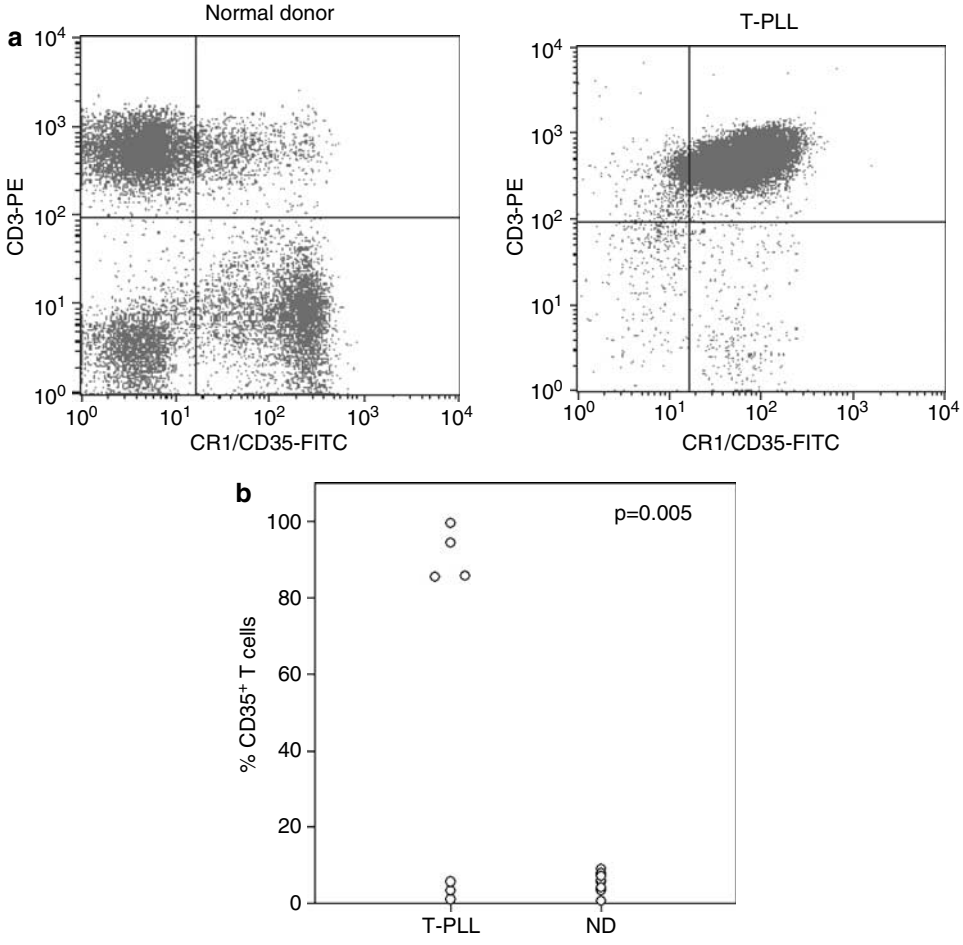

Figure 3 Flow cytometric analysis of CR1/CD35. CR1/CD35 expression on the surface of T-PLL ($n=7$) and normal donor (ND, $n=10$)-derived peripheral blood T cells was determined by two-color flow cytometry employing directly fluorochrome-labeled antibodies. (**a**) Representative dot-plot analyses of a T-PLL patient (T-PLL1) and a ND. (**b**) The relative density of CR1/CD35 on lymphocyte-gated CD3+ T cells was quantified by determining the mean fluorescent intensity (MFI) for FITC and subtracting the corresponding MFI values of the control antibody. The CR1/CD35 expression levels of individual T-PLL patients and healthy controls (ND) are plotted as geometric means. Statistical significance was determined using non-parametric Mann–Whitney *U*-test.

through increased expression of IGFBP5 and IGFBP7 (Supplementary Table 2) in T-PLL might promote leukemic cell growth.[30]

Of note, CR1 encoding complement component (3b/4b) receptor 1 (CD35) was found to be 18.6-fold upregulated in the T-PLL samples ($P=0.017$, Supplementary Table 2). Although

limited to a subset of 4/7 cases, differential surface expression of the CR1/CD35 protein was confirmed using multiparameter flow cytometry in a series of seven T-PLL samples where viably frozen cells were available for analysis vs 10 normal controls (Figure 3). Thus, CD35 could serve as a novel diagnostic marker in at least a subset of T-PLL.

Hypergeometric distribution analysis of GEP data. Testing the 830 probe sets differentially expressed between T-PLL and normal controls (Supplementary Table 2A) for nonrandom distribution to individual chromosomes using the 'hypergeometric distribution method'[23] revealed highly significant enrichment ($P \leqslant 0.01$) of upregulated genes on chromosome arms 6p and 8q and of downregulated genes on 6q, 8p, 10p, 11q and 18p (Table 1). Thus, at the chromosome-arm-specific-level clustering of deregulated genes is closely correlated with the typical pattern of chromosomal imbalances in T-PLL (Figure 1) and suggests 10p and 18p as novel potential targets in the pathogenesis of this T-cell neoplasm. In total, 186 of 830 differentially expressed probe sets (22%) were found to be significantly enriched in chromosomal regions shown to be affected by genomic aberrations secondary to inv(14)/t(14;14). Some of these candidate genes are involved in DNA repair (NBS1, ATM), regulation of apoptosis (CASP1, CASP4) and nucleosome assembly. Histone genes including HIST1H2AE, HIST1H2B, HIST1H4G may play an important functional role in disease progression and thus, could serve as interesting targets for the development of novel therapeutic agents.

Genome mapping using SNP-based arrays and FISH

Copy-number changes. To refine chromosomal aberrations associated with clustering of deregulated genes, Affymetrix GeneChip 50K SNP *Xba*I mapping array analyses were performed in a total of 11 T-PLL with inv(14)(q11q32) or t(14;14)(q11;q32), including those subjected to gene expression analyses, and one T-PLL case without inv(14)/t(14;14) (Supplementary Table 1). Recurrent regions of gains in 6p (3/12) and 8q (10/12) and of losses in 6q (5/12), 8p (7/12) and 11q (3/12) were usually large, ranging from 25.8 to 72.3 Mb in size (Table 2). In line with the enrichment of downregulated genes, novel regions of recurrent losses were detected in 10p (4/12 cases, minimal deleted region 3.2 Mb) and 18p (10.3 Mb) in 3/12 T-PLL (Tables 2 and 4). Three T-PLL cases carried the characteristic iso(8q) and six others a cytogenetically proven der(8p). High-resolution mapping of the breakpoints associated with loss of 8p and gain of 8q revealed scattering of the breakpoints over 7.2 Mb in 8p12–8p11.21 (34.6–41.8 Mb) (Figure 4), which is in line with previous reports.[31] Similar to chromosome 8, the breakpoints of the recurrent 6q− ($n=5$) scattered over two chromosomal regions of 27.8 and 37.9 Mb and the breakpoints of the typical dim/enh(22q) ($n=4$) over a region of 9 Mb. SNP array data compared favorably to FISH results with respect to copy number in the samples, with 28 of 32 SNP array tests matching FISH copy-number data (Supplementary Table 5).

Uniparental disomy. It has recently been shown that allelic loss may be caused by mechanisms other than loss of copy number.[32] Functional allelic loss occurs when one allele is deleted and the remaining dysfunctional allele is duplicated resulting in copy-number neutral loss of heterozygosity (LOH). Uniparental disomy (UPD) can be detected by SNP-mapping array technology and has recently been shown to play an important role in the molecular pathogenesis of various malignancies including acute myeloid leukemia and multiple myeloma.[15,32,33] Here, we defined partial UPD (pUPD) as a region spanning at least 50 SNPs with homozygous allele calls

Table 2 Summary of copy-number changes identified by SNP array

No.	*Chromosomal band*	*Deleted region, commonly deleted region (Mb)*	*No. of cases*
1	1p13.3-1p12	107.06–118.27	1
2	1q43	236.31–236.97	1
3	2p21	42.55–45.52	1
4	2q32.3-2q33.1	191.92–199.88	1
5	3p24.1	27.16–28.90	1
6	3p14.1-3p13	69.86–73.00	1
7	3q13.33-3q21.2	123.10–125.81	1
8	6p24.1-6p22.1	11.49–26.66	1
9	6q16.1-6q22.31	95.21–123.03	4
10	6q23.2-6q27	133.06–170.77	4
11	7q34-7q36.3	141.44–158.55	1
12	8p23.3-8p12	0.18–34.35	7
13	9p24.2-9p24.1	3.46–5.68	1
14	10p12.1-10p11.23	26.99–30.26	4
15	10p11.22-10p11.21	34.11–35.98	2
16	10q21.3	67.10–71.36	1
17	11p15.4-11p15.3	10.33–11.14	3
18	11p14.3	22.37–24.74	1
19	11p12-11p11.2	43.22–44.74	2
20	11q14.3-11q23.2	88.81–114.63	3
21	12p13.2-12p12.1	10.22–23.05	3
22	12p11.1-12q13.13	33.76–48.64	1
23	12q23.3-12q24.33	105.92–132.10	1
24	13q33.1-13q34	103.31–114.04	4
25	14q11.2	21.53–22.05	10
26	14q31.1	81.10–82.19	1
27	16p13.2	6.84–8.44	1
28	16p12.1	2.52–26.68	1
29	16q21-16q24.3	60.29–88.15	2
30	17p13.3-17p13.2	0.45–4.36	4
31	17q24.1-1725.3	61.58–78.18	1
32	18p11.23-18p11.22	0.15–10.36	3
33	18q12.1	24.63–24.65	2
34	18q21.31-18q21.32	53.65–56.32	2
35	18q22.1	62.03–64.00	2
36	18q22.3-18q23	69.48–72.32	2
37	20p12.1-20q12	14.73–41.00	2
38	21q21.1-21q22.2	16.29–40.99	2
39	22q11.21-22q12.3	16.93–35.16	2

No.	*Chromosomal band*	*Gained region, commonly gained region (Mb)*	*No. of cases*
1	2p25.2-2p25.1	4.65–7.92	1
2	2q11.2	98.8–102.00	1
3	3pter-3p14.1	0.01–70.45	1
4	3q12.2-3q23	102.18–141.68	1
5	4q28.3-4q35.2	139.02–191.09	4
6	5p15.33-5p15.2	0.01–11.91	2
7	6p22.1-6p12.1	27.94–57.39	3
8	7p14.1-7q11.23	43.21–77.40	1
9	8p12	29.96–30.73	1
10	8q12.3-8q24.3	62.57–143.90	10
11	11q24.1-11q25	122.00–131.63	1
12	13q13.3-13q14.13	37.83–46.02	1
13	14q22.2-14q23.2	53.84–62.72	2
14	14q31.3-14q32.33	84.03–106.0	2
15	16p13.3-16p13.2	6.00–6.72	1
16	16p13.13-16p12.13	11.73–19.20	1
17	16p12.1-16q21	26.80–60.24	1
18	17q21.31-17q25.3	41.10–78.18	1
19	19q13.32-19q13.43	51.27–63.44	2
20	20q13.13-20q13.2	46.36–50.20	1
21	whole chr21	chr21	1

Abbreviation: SNP, single nucleotide polymorphism.

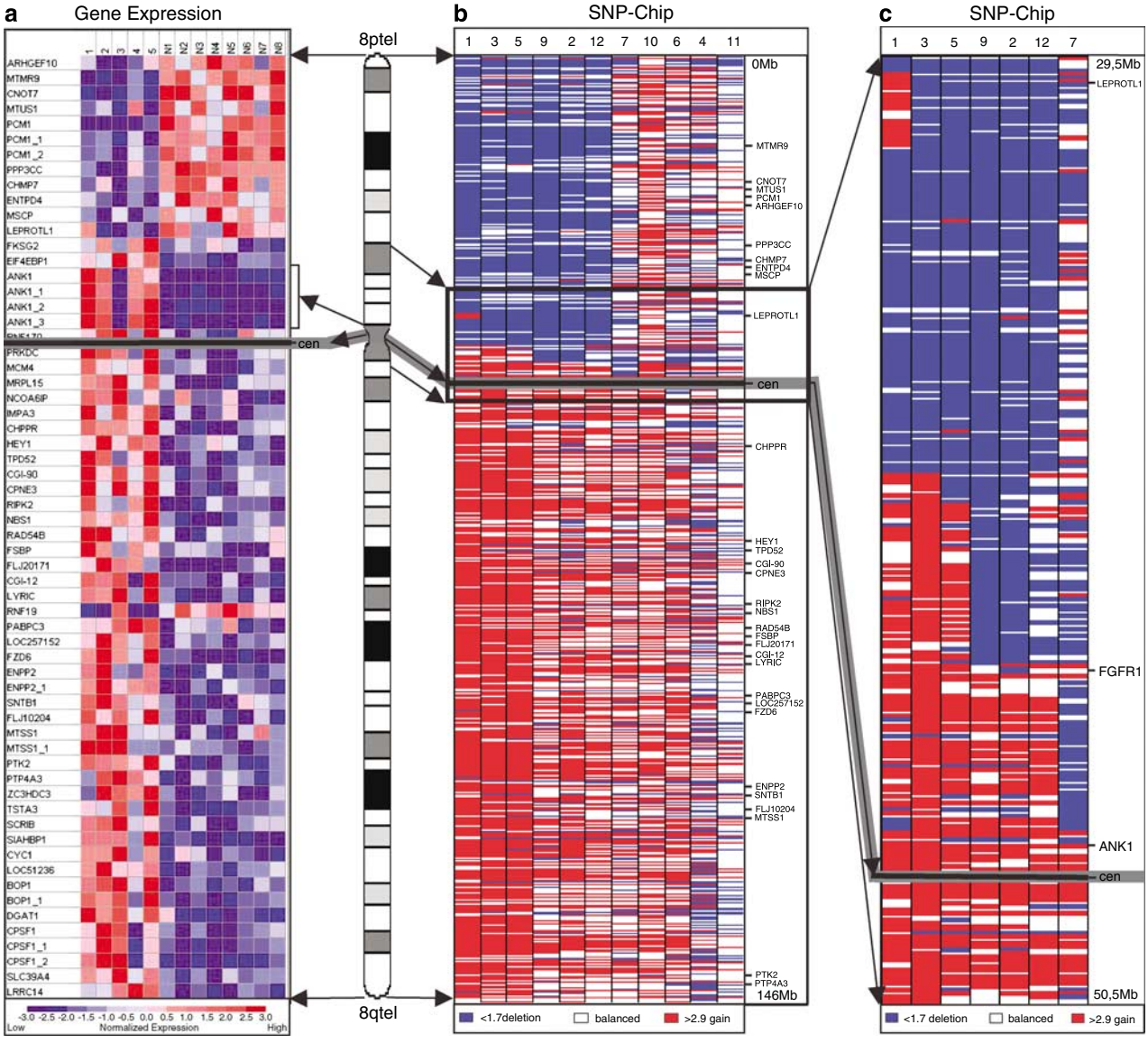

Figure 4 Integration of SNP-based genomic mapping and GEP of chromosome 8. (**a**–**c**) Correlation of GEP and SNP-chip data on chromosome 8. In both graphs, each column corresponds to one sample, each line to a tag. In the GEP graph, (**a**) only expression tags of significantly deregulated genes are shown and ordered from p-telomere to q-telomere. Significant downregulation of genes is shown in blue color, significant upregulation in red color. (**b**) Copy-number counts of the SNPs are lined up according to their chromosomal location. A loss of genomic material is marked in blue, a gain in red. Details of color coding are explained in the respective legends. Arrows indicate chromosomal location of tags. See legends to Supplementary Figure S2 and Supplementary Table 5 for a detailed description of evaluation and validation approaches. (**c**) Magnification of the breakpoint regions. Color coding is explained in the legend. Approximate chromosomal locations of the genes FGFR and ANK are highlighted. For supervised analyses, we employed non-parametric Mann–Whitney *U*-test (Affymetrix DMT tool). Filter criteria for the detection of differentially regulated genes are given in the legend to Supplementary Table 2.

and a $-\log_{10}$ (*P*-value) for LOH above 15 in the absence of a deletion.[34] Using these criteria, two cases showed an overlapping region of UPD in 3q (Table 3). There are eight non-recurrent regions of pUPD on chromosomes 3 (one region), 6 (four regions), 9, 11 and 13 (one region each). The average size of UPD is 4 Mb. It is interesting to note, that in five instances occurrence of pUPD was associated with a change in copy number on the same chromosome arm (Table 3).

Integration of SNP-based genomic mapping and GEP of chromosome 8

As described above and in previously published works,[3,6] alterations of chromosome 8 represent the most common aberration secondary to inv(14)/t(14;14) in T-PLL. Figure 4 gives an integrated overview of SNP chip ($N=11$) and GEP ($N=5$) results obtained from all of the samples with proven inv(14)/t(14;14) (Supplementary Table 1). In total, 62 of 830 (7.5%) probe sets found to be differentially expressed between T-PLL and ND-derived T-cell samples were located on chromosome 8 (Supplementary Table 2, Table 1). Interestingly, consistent with the loss of chromosomal material on 8p we found that the expression of the tumor suppressor gene MTUS1[35] was significantly downregulated as compared to normal controls. Also in accordance with the gain of chromosomal material, 40/41 differentially expressed genes located on 8q were found to be upregulated (Table 1). Potentially important, this set of genes included NBS1 or nibrin, the overexpression of which has

Table 3 Regions of pUPD in T-PLL

No.	*Chromosomal region*	*Size of UPD region (Mb)*	*No. of SNPs included*	*Chromosomal region of copy number change if present on the same chromosome arm*	*Case no.*
1	3q24-3q27.3	41.9	805	gain 3q12.2-3q23	5
2	3q26.1	3.7	102	n.c.	12
3	3q27.3-3q28	4.5	124	gain 3q12.2-3q23	5
4	6p24.1-6p22.3	3.5	81	loss 6p24.1-6p22.1	9
5	6p22.3	3.5	106	loss 6p24.1-6p22.1	9
6	6p22.1	3.3	93	n.c.	11
7	6p12.3-6p12.2	2.5	75	n.c.	7
8	9p21.1	1.4	88	n.c.	1
9	11q23.3-11q25	11.7	184	loss 11q13.1-11q23.2	2
10	13q21.1-13q21.2	3.4	81	n.c.	7

Abbreviations: LOH, loss of heterozygosity; n.c., no change of copy number; pUPD, partial uniparental disomy; SNP, single nucleotide polymorphism.
pUPD was defined as a region spanning at least 50 SNPs with homozygous allele calls and a $-\log_{10}$ (*P*-value) for LOH above 15 in the absence of a deletion.

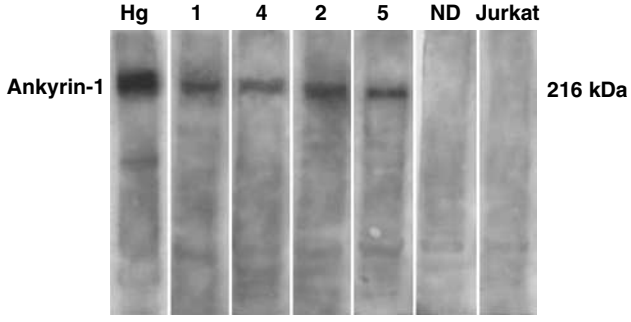

Figure 5 Immunoblot analysis of T-PLL cells for ankyrin-1 T-PLL cells, normal donor (ND) peripheral blood mononuclear cells (PBMNCs) and Jurkat cells were homogenized and analyzed for the presence of the erythrocytic membrane protein ankyrin-1. As a positive control human erythroid membranes (human ghosts, HG) were loaded on the left lane. Here the strong signal of a protein band represents ankyrin with its molecular weight of 216 kDa. The designation of T-PLL samples corresponds to Supplementary Table 1.

recently been shown to contribute to the oncogenic transformation of head and neck cancer and non-small cell lung cancer cells through the activation of the PI3/Akt pathway.[36–38] Furthermore, chromosome 8 aberrations were associated with aberrant expression of the erythrocytic structural membrane protein ankyrin-1, which was absent in the eight normal control samples and the T-PLL case lacking iso(8q) (see T-PLL 3 in Figure 4). Aberrant expression of ankyrin-1 was confirmed at the protein level using western blot (Figure 5).

Discussion

The advent of high-density SNP array technology allows for the high-resolution analysis of copy-number changes and copy-number neutral allelic loss caused by UPD. Combining SNP array-derived genomic information with data generated by gene expression arrays obtained from the same tumor samples provides a powerful tool for the identification of pathologically relevant genes.[15] Here, we applied this integrated SNP-based mapping and expression array approach to peripheral blood samples from patients with T-PLL defined by WHO diagnostic criteria[17] and the presence of inv(14)/t(14;14). Because of the rarity of the disease, our study was limited to tumor samples from a cohort of 12 patients (Supplementary Table 1). For all of these cases, viably frozen PBMNCs with a tumor cell content of >60% were available for DNA extraction and subsequent SNP-array analysis. However, due to technical considerations GEP was performed on fresh immunomagnetically purified tumor samples only and thus restricted to a subset of five tumor samples. Despite the small size of the study cohort, we observed highly significant changes in the gene expression profiles of T-PLL cells as compared to ND-derived T cells, thereby providing a focus for further studies of the molecular pathogenesis of this disease.

The primary oncogenic event in T-PLL appears to be an inversion or translocation of chromosome 14 that juxtapose enhancer elements of the TCRAD locus at 14q11 next to oncogenes located at 14q32, whose expression is then deregulated.[7,9] Work by Saitou *et al*.[39] and the Croce and co-workers[40] has identified the presence of four different candidate proto-oncogenes, that is TCL1A, TCL1B, TNG1 and TNG2, located in the breakpoint cluster region at 14q32. The most important of these is the TCL1A gene, which is consistently expressed in T-PLL with inv(14)/t(14;14), but not in normal T cells. Transgenic mouse studies have demonstrated that overexpression of TCL1 induces T-cell malignancies in these animals suggesting that TCL1 plays a causal role in the transformation process.[10] More recently, TCL1 was shown to physically interact with the Akt survival kinase which is then activated and translocated to the nucleus, which may explain at least in part the oncogenic potential of TCL1 at the molecular level.[41] Reassuringly, we found that TCL1A, but not TCL1B and TNG2, was highly expressed in the T-PLL samples, whereas it could not be detected in ND-derived T cells and a T-PLL case lacking inv(14)/t(14;14) (Figure 2). These findings support the concept of TCL1A being the primary oncogenic target of inv(14)(q11q32.1) in the T-PLL cases described here. However, it is interesting to note that one out of five T-PLLs but none of the normal controls also overexpressed TNG1 (Figure 2). This observation is in accordance with a study by Hallas *et al*.[40] suggesting that inv(14)/t(14;14) can induce the coordinate overexpression of other genes than TCL1A at 14q32 at least in some cases of T-PLL.[40] In their report, Saitou *et al*.[39] argued that TNG1 and TNG2 represent different isoforms of the TCL6 gene rather than independent genes. These authors suggest that TCL6 just as TCL1 could serve as a candidate oncogene involved in the malignant transformation of T cells.[39]

Besides the primary oncogenic aberration on chromosome 14, T-PLL cells usually harbor a high load of additional chromosomal abnormalities (Figure 1). The pattern of secondary

Table 4 Overview of deregulated genes in the critical regions with their localization and genomic alteration

	Chromosomal region with altered gene expression	*Hypergeometric analysis (P-value)*	*Chromosomal aberration (SNP chip)*	*Borders of minimally gained/lost regions by SNP chip (Mb from p-telomer)*	*Genes located in the minimal regions, significantly deregulated*
Significant accumulation of upregulated genes	chr8q	0.00001	Gain (10/12)	8q12.3 (62.6 Mb)–8qtel (143.9 Mb)	CHPPR, HEY1, TPD52, CGI-90, CPNE3, RIPK2, NBS1, RAD54B, FSBP/RAD54B, FLJ20171, CGI-12, LYRIC, PABPC3, LOC257152, FZD6, ENPP2, SNTB1, FLJ10204, MTSS1, PTK2, PTP4A3
	chr6p	0.000316	Gain (3/12)	6p22.1 (27.9 Mb)–6p12.1 (57.4 Mb)	HIST1H2AL, ZNF305, BPHL, IER3, DDR1, LST1, VARS2, AGPAT1, GPSM3, HSD17B8, RING1, PEX6, PPP2R5D, HSPCB, PRIM2A
Significant accumulation of downregulated genes	chr11q	0.00001	Loss (6/12)	11q14.3 (88.8 Mb)–11q23.2 (114.6 Mb)	BIRC3, CASP4, CASP1, CUL5, ACAT1, NPAT, ATM, RDX, DLAT, MGC5306, CRSP6, FGIF, SRP46, PIG8
	chr10p	0.00006	Loss (4/12)	10p12.1 (27.0 Mb)–10p11.23 (30.2 Mb)	YME1L1
	chr6q	0.000247	Loss (5/12)	6q16.1 (95.2 Mb)–6q22.31 (123.0 Mb) (4 cases), 6q23.2 (133.1 Mb)–6qtel (171.0 Mb) (4 cases)	PRDM1, AIM1, MICAL1, FYN, C6orf61, MAN1A1, HSF2, TDE2, C6orf75, HBS1L, MAP3K5, PHACTR2, MAP3K7IP2, SYNE1, TCTEL1, ATXN1, C6orf111
	chr18p	0.00031	Loss (3/12)	18ptel (0 Mb)–18p11.22 (10.3 Mb)	THOC1, ENOSF1, PTPRM, NDUFV2, ANKRD12
	chr8p	0.010818	Loss (7/12)	8ptel (0 Mb)–8p12 (35.0 Mb)	MTMR9, CNOT7, MTUS1, PCM1, ARHGEF10, PPP3CC, CHMP7, ENTPD4, MSCP, LEPROTL1

Abbreviation: SNP, single nucleotide polymorphism.
Borders for minimally gained/lost regions were determined according to the March 2006 human reference sequence (NCBI Build 36.1) of the International Human Genome Sequencing Consortium.

chromosomal changes detected by SNP array in this study (Table 2) tallies well with previously reported data sets.[3,6] Of note, in addition to the known characteristic chromosomal imbalances shown in Figure 1, we observed as yet undescribed novel recurrent aberrations affecting 10p and 18p. More importantly, hypergeometric distribution analysis of GEP data revealed that 22% of the probe sets found to be differentially expressed between T-PLL and normal T cells map to chromosomal regions affected by recurrent imbalances occurring secondary to inv(14)/t(14;14) (Table 1). Some of these candidate genes are involved in DNA repair (ATM, DLCRE1C), regulation of apoptosis (CASP1, CASP4) and nucleosome assembly. Several histone genes (Supplementary Table 2 and Table 4) found to be overexpressed due to a gain of chromosomal material on 6p may play an important functional role in disease progression and thus could serve as interesting targets for the development of novel therapeutic agents. The short arm of chromosome 8 is a frequent target of genetic alterations in a wide variety of human cancers[42] including breast cancer[43] and T-PLL.[3,6] We found that T-PLL cases exhibiting a DNA amplification at 8p11.1 aberrantly express the erythrocytic structural membrane protein ankyrin-1 both at the mRNA and protein level. Ankyrins are a family of proteins that are believed to link the integral membrane proteins to the underlying spectrin-actin cytoskeleton and play key roles in activities such as cell motility, activation, proliferation, contact and the maintenance of specialized membrane domains.[27,44] It is thus tempting to speculate that aberrant expression of this molecule may contribute to the abnormal migratory behavior of T-PLL cells as evidenced by the commonly observed tumor cell infiltration of the skin and peritoneal cavity.[2]

Even more strikingly, we observed a highly significant 2.3-fold overexpression of the NBS1/nibrin gene in T-PLL samples with a gain of chromosomal material on 8q as compared to normal controls (Figure 4). Increased NBS1 expression has been observed in non-small cell lung carcinoma, hepatoma, melanoma and esophageal cancer samples.[36–38] Furthermore, Chen *et al*.[36] have recently demonstrated that constitutive expression of NBS1 in Rat1a and HeLa cells induces/enhances their transformation through stimulation of phosphatidylinositol (PI)3-kinase activity, leading to increased phosphorylation levels of Akt and its downstream targets such as mammalian target of rapamycin. It is thus tempting to speculate that increased NBS1 expression contributes to TCL1-induced enhanced Akt signaling in T-PLL cells, which has been suggested to be causal for disease progression.[41]

Copy-number neutral LOH (UPD) is increasingly recognized as an important genetic mechanism in cancer biology where silencing of tumor suppressor genes may play a role in the transformation process and disease progression.[15,32] Here, we describe for the first time the occurrence of pUPD in 7 out of 11 T-PLL cases analyzed by SNP-array technology. We found eight non-recurrent regions of pUPD interspersed throughout the genome predominantly affecting chromosome 6 (four regions), and identified two cases showing an overlapping region of pUPD in 3q (Table 3). Interestingly, in 5 out of 10 instances, pUPD was associated with a copy-number change observed on the same chromosome arm suggesting that the genetic mechanisms underlying these abnormalities may be linked. The detection of UPD in T-PLL raises the possibility of identifying functionally important genes that are downregulated through epigenetic mechanisms or mutations but retain a

diploid copy number. In this context, a combined SNP array and global GEP approach could provide a useful tool to identify such candidate genes. Unfortunately, in our present study, the small number of cases analyzed by both GEP and SNP array ($N=5$) precluded a meaningful analysis of gene expression changes in regions affected by pUPD.

In conclusion, comparative transcriptional and molecular cytogenetic profiling in T-PLL with inv(14)(q11q32) demonstrates that a substantial number of the deregulated genes map to genomic regions targeted by recurrent chromosomal aberrations suggesting that a gene dosage effect may play a role in the disease process (Table 4). The upregulated expression of genes involved in chromatin composition and PI3K/Akt signaling detected in the present study along with ATM defects might point to a pathogenic role of altered DNA repair, nucleosome assembly and cell survival. Finally, we have identified novel regions of recurrent chromosomal imbalances and candidate genes, providing a focus for further studies addressing the molecular pathogenesis and novel treatment strategies in T-PLL.

Acknowledgements

We thank Anja Führer, Ute Schmücker, Reina Zühlke-Jenisch, Doris Schuster and Claudia Becher for excellent technical assistance and numerous colleagues for contributing patient samples and information on their clinical course and treatment histories. This work is dedicated to Professor G Brittinger on the occasion of his 75th birthday.

References

1 Herling M, Khoury JD, Washington LT, Duvic M, Keating MJ, Jones D. A systematic approach to diagnosis of mature T-cell leukemias reveals heterogeneity among WHO categories. *Blood* 2004; **104**: 328–335.
2 Matutes E, Brito-Babapulle V, Swansbury J, Ellis J, Morilla R, Dearden C *et al*. Clinical and laboratory features of 78 cases of T-prolymphocytic leukemia. *Blood* 1991; **78**: 3269–3274.
3 Soulier J, Pierron G, Vecchione D, Garand R, Brizard F, Sigaux F *et al*. A complex pattern of recurrent chromosomal losses and gains in T-cell prolymphocytic leukemia. *Genes Chromosomes Cancer* 2001; **31**: 248–254.
4 Dearden CE, Matutes E, Cazin B, Tjonnfjord GE, Parreira A, Nomdedeu B *et al*. High remission rate in T-cell prolymphocytic leukemia with CAMPATH-1H. *Blood* 2001; **98**: 1721–1726.
5 Dearden CE. T-cell prolymphocytic leukemia. *Med Oncol* 2006; **23**: 17–22.
6 Brito-Babapulle V, Pomfret M, Matutes E, Catovsky D. Cytogenetic studies on prolymphocytic leukemia. II. T cell prolymphocytic leukemia. *Blood* 1987; **70**: 926–931.
7 Croce CM. Role of chromosome translocations in human neoplasia. *Cell* 1987; **49**: 155–156.
8 Pekarsky Y, Hallas C, Croce CM. The role of TCL1 in human T-cell leukemia. *Oncogene* 2001; **20**: 5638–5643.
9 Pekarsky Y, Hallas C, Croce CM. Molecular basis of mature T-cell leukemia. *JAMA* 2001; **286**: 2308–2314.
10 Virgilio L, Lazzeri C, Bichi R, Nibu K, Narducci MG, Russo G *et al*. Deregulated expression of TCL1 causes T cell leukemia in mice. *Proc Natl Acad Sci USA* 1998; **95**: 3885–3889.
11 Stankovic T, Taylor AMR, Yuille MR, Vorechovsky I. Recurrent ATM mutations in T-PLL on diverse haplotypes: no support for their germline origin. *Blood* 2001; **97**: 1517–1518.
12 Stilgenbauer S, Schaffner C, Litterst A, Liebisch P, Gilad S, BarShira A *et al*. Biallelic mutations in the ATM gene in T-prolymphocytic leukemia. *Nat Med* 1997; **3**: 1155–1159.
13 Schoch C, Kohlmann A, Dugas M, Kern W, Hiddemann W, Schnittger S *et al*. Genomic gains and losses influence expression levels of genes located within the affected regions: a study on acute myeloid leukemias with trisomy 8, 11, or 13, monosomy 7, or deletion 5q. *Leukemia* 2005; **19**: 1224–1228.
14 Staudt LM. Molecular diagnosis of the hematologic cancers. *New Engl J Med* 2003; **348**: 1777–1785.
15 Walker BA, Leone PE, Jenner MW, Li C, Gonzalez D, Johnson DC *et al*. Integration of global SNP-based mapping and expression arrays reveals key regions, mechanisms, and genes important in the pathogenesis of multiple myeloma. *Blood* 2006; **108**: 1733–1743.
16 Haslinger C, Schweifer N, Stilgenbauer S, Dohner H, Lichter P, Kraut N *et al*. Microarray gene expression profiling of B-cell chronic lymphocytic leukemia subgroups defined by genomic aberrations and VH mutation status. *J Clin Oncol* 2004; **22**: 3937–3949.
17 Jaffe ES, Harris N, Stein H, Vardiman JW. *Tumours of Hematopoietic and Lymphoid Tissues. WHO Classification of Tumours*. IARC Press: Lyon, 2001.
18 Baudis M, Cleary ML. Progenetix.net: an online repository for molecular cytogenetic aberration data. *Bioinformatics* 2001; **17**: 1228–1229.
19 Baudis M. Online database and bioinformatics toolbox to support data mining in cancer cytogenetics. *Biotechniques* 2006; **40**: 269–270.
20 Schroers R, Griesinger F, Trumper L, Haase D, Kulle B, Klein-Hitpass L *et al*. Combined analysis of ZAP-70 and CD38 expression as a predictor of disease progression in B-cell chronic lymphocytic leukemia. *Leukemia* 2005; **19**: 750–758.
21 Wu B. Differential gene expression detection using penalized linear regression models: the improved SAM statistics. *Bioinformatics* 2005; **21**: 1565–1571.
22 Beissbarth T, Speed TP. GOstat: find statistically overrepresented gene ontologies within a group of genes. *Bioinformatics* 2004; **20**: 1464–1465.
23 Tavazoie S, Hughes JD, Campbell MJ, Cho RJ, Church GM. Systematic determination of genetic network architecture. *Nat Genet* 1999; **22**: 281–285.
24 Martin-Subero JI, Harder L, Gesk S, Schlegelberger B, Grote W, Martinez-Climent JA *et al*. Interphase FISH assays for the detection of translocations with breakpoints in immunoglobulin light chain loci. *Int J Cancer* 2002; **98**: 470–474.
25 Mitelman F. *ISCN: an International System for Human Cytogenetic Nomenclature*. Karger: Basel, 1995.
26 Matsuzaki H, Dong S, Loi H, Di X, Liu G, Hubbell E *et al*. Genotyping over 100 000 SNPs on a pair of oligonucleotide arrays. *Nat Methods* 2004; **1**: 109–111.
27 Jöns T, Drenckhahn D. Anion exchanger 2 (AE2) binds to erythrocyte ankyrin and is colocalized with ankyrin along the basolateral plasma membrane of human gastric parietal cells. *Eur J Cell Biol* 1998; **75**: 232–236.
28 De Schouwer PJJC, Dyer MJS, Brito-Babapulle VB, Matutes E, Catovsky D, Yuille MR. T-cell prolymphocytic leukaemia: antigen receptor gene rearrangement and a novel mode of MTCP1 B1 activation. *Br J Haematol* 2000; **110**: 831–838.
29 Padovan E, Casorati G, Dellabona P, Meyer S, Brockhaus M, Lanzavecchia A. Expression of 2 T-cell receptor-alpha chains – dual receptor T-cells. *Science* 1993; **262**: 422–424.
30 Vorwerk P, Wex H, Hohmann B, Mohnike K, Schmidt U, Mittler U. Expression of components of the IGF signalling system in childhood acute lymphoblastic leukaemia. *J Clin Pathol Mol Pathol* 2002; **55**: 40–45.
31 Sorour A, Brito-Babapulle V, Smedley D, Yuille M, Catovsky D. Unusual breakpoint distribution of 8p abnormalities in T-prolymphocytic leukemia: a study with YACS mapping to 8p11-p12. *Cancer Genet Cytogenet* 2000; **121**: 128–132.
32 Raghavan M, Lillington DM, Skoulakis S, Debernardi S, Chaplin T, Foot NJ *et al*. Genome-wide single nucleotide polymorphism analysis reveals frequent partial uniparental disomy due to somatic recombination in acute myeloid leukemias. *Cancer Res* 2005; **65**: 375–378.
33 Murthy SK, DiFrancesco LM, Ogilvie RT, Demetrick DJ. Loss of heterozygosity associated with uniparental disomy in breast carcinoma. *Mod Pathol* 2002; **15**: 1241–1250.
34 Nielaender I, Martin-Subero JI, Wagner F, Martinez-Climent JA, Siebert R. Partial uniparental disomy: a recurrent genetic mechan-

ism alternative to chromosomal deletion in malignant lymphoma. *Leukemia* 2006; **20**: 904–905.
35 Di Benedetto M, Bieche I, Deshayes F, Vacher S, Nouet S, Collura V *et al*. Structural organization and expression of human MTUS1, a candidate 8p22 tumor suppressor gene encoding a family of angiotensin II AT2 receptor-interacting proteins, ATIP. *Gene* 2006; **380**: 127–136.
36 Chen YC, Su YN, Chou PC, Chiang WC, Chang MC, Wang LS *et al*. Overexpression of NBS1 contributes to transformation through the activation of phosphatidylinositol 3-kinase/Akt. *J Biol Chem* 2005; **280**: 32505–32511.
37 Ehlers JP, Harbour JW. NBS1 expression as a prognostic marker in uveal melanoma. *Clin Cancer Res* 2005; **11**: 1849–1853.
38 Yang MH, Chiang WC, Chou TY, Chang SY, Chen PM, Teng SC *et al*. Increased NBS1 expression is a marker of aggressive head and neck cancer and overexpression of NBS1 contributes to transformation. *Clin Cancer Res* 2006; **12**: 507–515.
39 Saitou M, Sugimoto J, Hatakeyama T, Russo G, Isobe M. Identification of the TCL6 genes within the breakpoint cluster region on chromosome 14q32 in T-cell leukemia. *Oncogene* 2000; **19**: 2796–2802.
40 Hallas C, Pekarsky Y, Itoyama T, Varnum J, Bichi R, Rothstein JL *et al*. Genomic analysis of human and mouse TCL1 loci reveals a complex of tightly clustered genes. *Proc Natl Acad Sci USA* 1999; **96**: 14418–14423.
41 Pekarsky Y, Koval A, Hallas C, Bichi R, Tresini M, Malstrom S *et al*. Tcl1 enhances Akt kinase activity and mediates its nuclear translocation. *Proc Natl Acad Sci USA* 2000; **97**: 3028–3033.
42 Emi M, Fujiwara Y, Nakajima T, Tsuchiya E, Tsuda H, Hirohashi S *et al*. Frequent loss of heterozygosity for loci on chromosome 8p in hepatocellular carcinoma, colorectal cancer, and lung cancer. *Cancer Res* 1992; **52**: 5368–5372.
43 Gelsi-Boyer V, Orsetti B, Cervera N, Finetti P, Sircoulomb F, Rouge C *et al*. Comprehensive profiling of 8p11-12 amplification in breast cancer. *Mol Cancer Res* 2005; **3**: 655–667.
44 Hryniewicz-Jankowska A, Czogalla A, Bok E, Sikorsk AF. Ankyrins, multifunctional proteins involved in many cellular pathways. *Folia Histochem Cytobiol* 2002; **40**: 239–249.

Supplementary Information accompanies the paper on the Leukemia website (http://www.nature.com/leu)